Automotive Science and Engineering, Vol. 12, No. 2, (2022), 3873-3880

Iran University of Science and Technology

Automotive Science and Engineering

Journal Homepage: ase.iust.ac.ir

ISSN: 2008-9899

Forming limit curves and mechanical properties for AA6061 sheet after solution treatment and during ageing

Majid Fallah Tafti [1], Ramin Hashemi [1, *], Mohammad Sedighi [1]

[1] School of Mechanical Engineering, Iran University of Science and Technology

ARTICLE INFO

Article history:
Received: 22 Aug 2020
Accepted: 27 Jun 2022
Published: 5 Jul 2022

Keywords:
Mechanical properties
Ageing
Forming limit curves
Solution
Sheet

A B S T R A C T

This paper aims to examine the influences of heat treatment on forming limit diagrams and mechanical properties of aluminum alloy AA6061 sheets with thicknesses of 1.5 mm. The uniaxial tensile and the micro-hardness tests are employed to specify the mechanical properties and their variations. The Nakazima test is performed to characterize the strain forming limits of this aluminum alloy. Comparison between the results of micro-hardness and forming limit diagrams indicates that by increasing the temperature up to the peaked ageing temperature, the strength of the alloy is increased, but the forming limits are decreased, and after the peaked aged in over the aged state, the strength is decreased and the forming limits are increased. The peaked-aging is touched in this specific alloy after 4 hours heat treatment at 180 oC.

*Corresponding Author
Email Address: rhashemi@iust.ac.ir
https://doi.org/10.22068/ase.2022.554

"*Automotive Science and Engineering*" is licensed under a Creative Commons Attribution-Noncommercial 4.0 International License.

[Downloaded from i4c2023.iust.ac.ir on 2026-11-21]

[DOI: 10.22068/ase.2022.554]

1. Introduction

6xxx aluminum alloys have been investigated widely because of their advantages such as medium strength, weld-ability, formability, corrosion resistance, and low expense, in comparison to other aluminum alloys [1,2]. These metals are heat treated to make precipitation to different grades [3-6]. Forming limit diagram (FLD), is based on the critical major and minor strains, it is also a tool for assessing formability of sheets [7]. FLDs are strong tools which are utilized to investigate the formability of sheet metals. They demonstrated the capability of a sheet to tolerate drawing and stretching [8].

Gunduz and Demir [9] examined the machinability of aged AA6061 in the initial condition, solution heat treated and aged conditions. By aging at the 180 ºC for different aging time, the cutting speed considerably affected the surface roughness values. Also, aging had a little effect on cutting force and cutting speed except for solution heat treated work-pieces having the lowest hardness. Ozturk et al. [10] characterized AA6061 aluminum alloy considering mechanical properties during aging treatment. Peak-aged conditions were reached after a 2 h and 200 °C. The changing of elongation, strain hardening rate, ultimate tensile strength and yield stress with aging time was determined and Interpreted referring to the microstructural alterations made by the aging treatment. Tan et al. [11] studied the AA 6061-T6 precipitation and the effects of temperatures (artificial ageing) of 175ºC to 420ºC on its hardness at different period of time. They showed that the optimum aged temperature was 175ºC to 195ºC with 2 to 6 hours of ageing time. Moy et al. [12] examined the influence of heat treatment on the formability, microstructure and texture of AA2024 sheets with thicknesses of 1.27 mm and 2.03 mm. The sheet forming limits were obtained by carrying out stretch forming tests. The microstructure observation using transmission electron microscopy (TEM) performed to the precipitation creation degrees at the different ageing times. AH1 (2 days) and AH2 (2.5 h) illustrated enhancement in elongation and a drop in mechanical strength in comparing to the as-received state (T3). AH3 (a week) showed the maximum strength and the minimum elongation as attended due to the peak-ageing condition. Their formability investigation demonstrated that AH2 had higher formability in plane strain mode than all the other modes. This phenomenon made it the best condition for sheet metal forming processes, since the critical strain conditions for stamping were mostly seen in plane strain mode. However, no study has noticed the effect of aging steps on alloy AA6061 that has high usage between aluminum alloys. According to the literature review, it can be seen that some attempts have been made to study the influences of aging treatment on mechanical properties of AA6061. However, according to the knowledge of the authors, forming limit diagrams for AA6061 sheet after solution treatment and during aging have not yet been determined.

In this article, mechanical properties and FLDs of Al-Mg-Si alloy (AA6061) sheets after solution and during aging heat treatment were determined experimentally for the first time. For this purpose, solution treatment was carried out first and after that aging treatment was performed at different temperatures. Sheet metal formability by referencing to the FLD, micro-hardness and mechanical properties were investigated after each step.

2. Experiment

2.1. Material

Aluminum alloy AA6061-T6 sheets of 1.5 mm thickness was utilized. For commencement, the material was cut to prepare specimens. The chemical composition (in wt. %) of AA6061 has been identified by quantometery examination and is informed in Table 1.

Table. 1. The chemical composition (in wt. %) of AA6061

Al	Mg	Mn	Fe	Si	Cr	Cu	Other
Balance	0.995	0.068	0.568	0.486	0.237	0.189	0.098

2.2. Heat treatment process

[Downloaded from i4c2023.iust.ac.ir on 2026-11-21]

[DOI: 10.22068/ase.2022.554]

Mechanism of precipitation hardening was performed on an AA6061 sheet (cold rolled sheet) with thickness of 1.5 mm. The sheets were solution treated at 530°C for 35 minutes [13] and age-hardened for different temperatures at a constant time (4 hour). The aging treatment process is displayed in Fig. 1.

The hardness was measured after solution and different aging temperatures. A Jenus Vickers was used with 200 g load and 10 seconds dwell time. We also performed the uniaxial tensile tests using a Galdabini 60 KN testing machine.

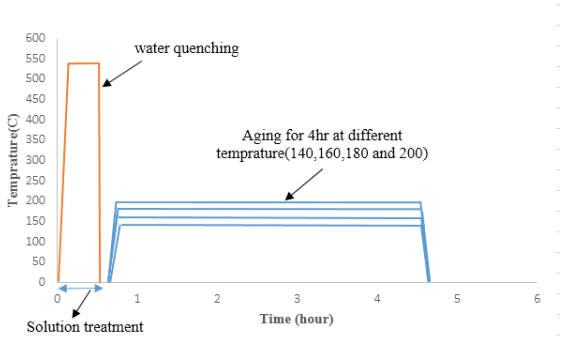


Fig. 1. The heat treatment process diagram.

2.3. Forming limit curves

We utilized the Nakazima test for determining the forming limit curves or FLDs. A schematic of the Nakazima test setup is shown in Fig. 2. The tests were performed in accordance with ISO 12004 for the both sides of FLD. The electro-chemical technique was used to mark the circular grids with 2.5 mm diameter on the surface of samples. A 5-ton constant speed, Santam STM-50 machine was employed for stretching samples. We considered the load–displacement diagram as the ending criterion in the test. We repeated the tests for the samples with different geometries. Fig. 3 shows the geometries of the samples to determine forming limit curve [14]. The samples after tests were shown in Fig. 4. The rounded grids have been changed to elliptic forms after experiments. The minor and major engineering strains were calculated by relations (1) and (2):

$$\varepsilon_{major}(\%) = \frac{a-d}{c} * 100 \qquad (1)$$

$$\varepsilon_{minor}(\%) = \frac{b-d}{c} * 100 \qquad (2)$$

Where b, a and c demonstrate the ellipse's minor and major diameters and the initial circle diameter [15]. Then, the engineering strains were converted into the true strains.

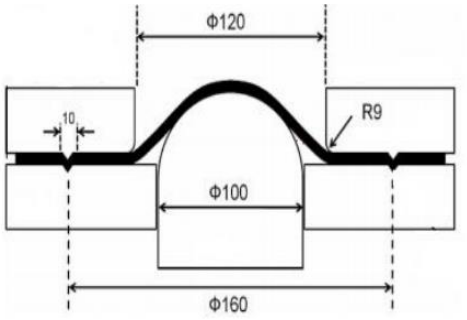


Fig. 2. The schematic view of setup for FLDs determination

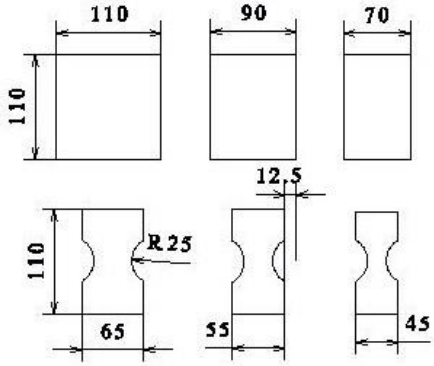


Fig. 3. The specimens geometry to obtain the forming limit curves (all the dimensions are in mm) [14]



Fig. 4. The typical deformed specimens

[Downloaded from i4c2023.iust.ac.ir on 2026-11-21]

[DOI: 10.22068/ase.2022.554]

3. Results and Discussion

3.1. Mechanical properties

A Galdabini 60 KN testing apparatus was utilized to accomplish the uniaxial-tensile tests. The material and mechanical properties were achieved using sub-size samples that were defined in the standard ASTM-E08/09, at a fixed speed of 3 mm/min. The stress-strain curves accomplished from the uniaxial tests for solution and aged samples were shown in Fig. 5. By increasing the aging temperature at constant time, the ultimate strength and yield strength were improved, while the elongation was reduced. For the various temperatures, fluctuations in the elongation at break, the ultimate strength, and the yield strength are demonstrated in Fig. 6. From solution up to coming to peak aged, the ultimate tensile strength (UTS) and the yield strength (YS) were boosted from 62 to 269 MPa and from 173 to 306 MPa, respectively.

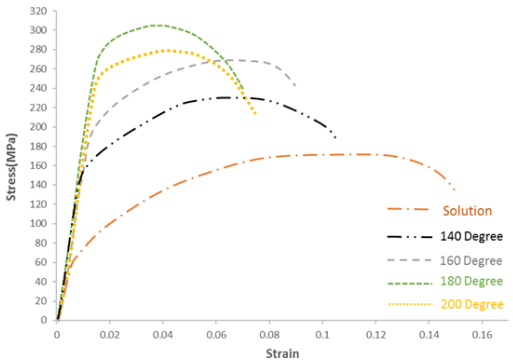


Fig. 5. The true stress-strain curves for heat treated specimens

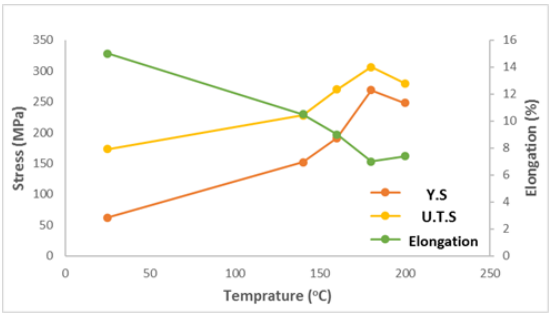


Fig. 6. The changes in the elongation at break, ultimate strength, yield strength based on the heat-treated specimens

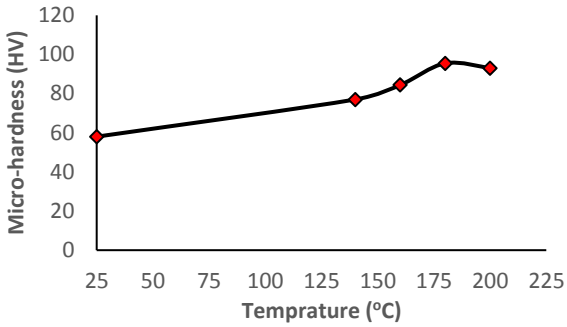


Fig. 7. Changes in the micro-hardness based on changing aging temperature

3.2. Micro-Hardness examination

We measured the micro-hardness variations in the heat-treated samples (e.g., see Fig. 7). It is obvious that after the aging treatment, hardness increased significantly, and in the maximum hardness (180 °C) an approximate 64% increase was illustrated in comparison with the solution samples. This variation is related to the microstructural evolutions.

The formation of Si co-clusters and Mg created initially. This caused hardness and yield stress, to increase slowly. Peaked-aging is related to a luxuriant population of β needle-shaped precipitates set in the $<100>_{Al}$ crystal directions, which seem to be desirable obstacles for dislocations [7], [9]. Some segments of precipitates stay in the microstructure in over the aging condition as the metastable phases, such as B' and β', form. The hardness and yield stress improve rapidly with aging temperature, and the total shape of the stress–strain curves vary as be seen in Fig. 5. Consistent with Fig. 6 the ultimate and yield strength follows an opposite behaviour to the elongation. Each aging step formability was assessed by determining the elongation at break.

The mentioned parameters are changed seldom for over-aged metals. The elongation at break is firstly (solution) 15%, 7% for peaked-aging, and 7.4% for over-aging conditions. Two diverse views were achieved from the results. We can shape the material first and after that aged or we can age the sheet first and then shaped. However, we can decide according to the application [10].

[Downloaded from i4c2023.iust.ac.ir on 2026-11-21]

[DOI: 10.22068/ase.2022.554]

3.3. FLD examination

The forming limit curves were determined for five various temperatures (Fig. 8) after calculating all true limit strains. We can see the FLDs after solution treatment in Fig. 8. The maximum forming limits of AA6061 were reached in this circumstance. The FLD_o for this condition is about 0.16. Fig. 8 is also representing the forming limit curve for aging at the temperature 140 ºC for 4 hours. The FLD_o for this case is about 0.12 that shows a 33% decrease compared to solution treatment. Fig. 8 also shows the FLD for temperature 160 ºC for same aging time. The FLD_o for this state is about 0.1 that reduced 20% linked to prior state (140 ºC). The FLD for peak-aged state could be seen in Fig. 8.

In this case, the lowest formability was achieved and it could be seen the brittle fracture on the sheet, whereas for solution state, there could be observed soft fracture and the necking was obviously observed. At peak-aged condition the specimen was experienced brittle fracture without necking. The FLD_o in this state is 0.06 and compared to the prior, has been experiencing a significant decrease the cause of which is a complete brittle fracture that happened in this state. Fig. 8 also displays the FLD in 200 ºC that happened with over-aging in this case. The FLD_o in this temperature is 0.065 that in comparison to the last state (peak-aged), the variation is insignificant. This insensible alteration is related to presence of β" phase in both conditions (peak-aged and over-aged) and similarity of β' and β" phases mechanical behaviors [10].

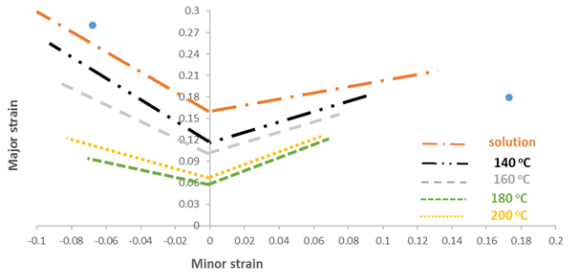


Fig. 8. The FLDs for all heat treatment conditions

Table. 2. The mechanical properties and FLDo of AA 6061

Sample	Micro-hardness (HV)	Ultimate Tensile Strength, (MPa)	Yield Strength, (MPa)	FLD_o	Elongation at Break, %
Solution	58	173	62	0.16	15
Aging at 140	77	140	152	0.12	10.5
Aging at 160	84.4	270	191	0.105	9
Aging at 180	95.5	306	269	0.6	7
Aging at 200	93	280	248	0.64	7.4

The R-value has a direct relation with forming limit curve, and different studies have been done to investigate the influence of this parameter on forming limit curve [16-18]. Habibi et al. [19], proved that by increasing the strength, the R-value decreased and it affected the left and right side of the FLDs. They demonstrated that increasing in strength and decreasing the R-value had a positive influence on forming limits in the right side and the enhancement of forming limits in the left side was rather lower. That it means by decreasing the R-value the curve slope in the right-hand side had more increasing than the left-hand side of the FLD. Also, Ozturk et al. [20] studied the effect of anisotropy in three directions- 0º, 45º and 90º on AA6061 sheets. They illustrated that in the rolling direction by increasing aging time and strength, the r-value decreased. According to Fig. 8 in comparison between aging conditions for solution treatment, the slop of the curves in the right-hand side of the FLDs is more than the left-hand side of the FLDs that the cause is decreasing in R-value. Table. 2 demonstrates all forming and mechanical properties of AA6061. The present work shows a new result comparing with the previous articles [20-26] that refer to forming limit diagram of AA6061.

[Downloaded from i4c2023.iust.ac.ir on 2026-11-21]
[DOI: 10.22068/ase.2022.554]

4. Conclusions

The present article studied how aging heat treatment effects the mechanical properties and formability of AA6061 sheets. The achieved results are as follows:

- Maximum strength (Peak-aging) case was attained by 4 hours aging at 180 ^{o}C. It is thought different Mg/Si atomic ratios would show a different temperature and a different time to maximum strength. And, also maximum elongation has been reached for just a little after solutioning (15%).
- Hardness and strength were increased during the aging treatment to peak-aging condition (76% increasing in UTS and 64% in hardness) and after that, both of them were decreased slightly.
- By comparing the FLD_o points from pre-aging state to peak-aging, it showed a significant decrease (about 75%) that affected by brittle fracture which occurred during peak-aging condition, and by passing the peak to over-aging case the variation was partial (about 6%).

References

[1] L. P. Troeger and E. S. Jr, "Microstructural and mechanical characterization of a superplastic 6xxx aluminum alloy," *Mater. Sci. Eng. A*, vol. 277, no. 1–2, pp. 102–113, 2000.

[2] S. Abis, a Boeuf, R. Caciuffo, P. Fiorini, M. Magnani, S. Melone, F. Rustichelli, and M. Stefanon, "Investigation of Mg2Si Precipitation in an Al-Mg-Si Alloy by Small-Angle Neutron-Scattering," *J. Nucl. Mater.*, vol. 135, no. 2–3, pp. 181–189, 1985.

[3] J. Buha, R. N. Lumley, a. G. Crosky, and K. Hono, "Secondary precipitation in an Al-Mg-Si-Cu alloy," *Acta Mater.*, vol. 55, no. 9, pp. 3015–3024, 2007.

[4] L. Zhen, W. D. Fei, S. B. Kang, and H. W. Kim, "Precipitation behaviour of Al-Mg-Si alloys with high silicon content," *J. Mater. Sci.*, vol. 32, no. 7, pp. 1895–1902, 1997.

[5] M. Murayama, K. Hono, M. Saga, and M. Kikuchi, "Atom probe studies on the early stages of precipitation in Al-Mg-Si alloys," *Mater. Sci. Eng. a-Structural Mater. Prop. Microstruct. Process.*, vol. 250, no. 1, pp. 127–132, 1998.

[6] C. D. Marioara, S. J. Andersen, J. Jansen, and H. W. Zandbergen, "The influence of temperature and storage time at RT on nucleation of the β" phase in a 6082 Al-Mg-Si alloy," *Acta Mater.*, vol. 51, no. 3, pp. 789–796, 2003.

[7] S. P. Keeler and W. A. Backofen, "Plastic instability and fracture in sheets stretched over rigid punches," *Asm Trans Q*, vol. 56, no. 1, pp. 25–48, 1963.

[8] D. W. a Rees, "Factors influencing the FLD of automotive sheet metal," *J. Mater. Process. Technol.*, vol. 118, no. 1–3, pp. 1–8, 2001.

[9] H. Demir and S. Gündüz, "The effects of aging on machinability of 6061 aluminium alloy," Mater. Des., vol. 30, pp. 1480–1483, 2009.

[10] F. Ozturk, A. Sisman, S. Toros, S. Kilic, and R. C. Picu, "Influence of aging treatment on mechanical properties of 6061 aluminum alloy," *Mater. Des.*, vol. 31, no. 2, pp. 972–975, 2010.

[11] C. F. Tan and M. R. Said, "Effect of hardness test on precipitation hardening aluminium alloy 6061-t6," *Chiang Mai J. Sci.*, vol. 36, no. 3, pp. 276–286, 2009.

[12] C. K. S. Moy, M. Weiss, J. Xia, G. Sha, S. P. Ringer, and G. Ranzi, "Influence of heat treatment on the microstructure, texture and formability of 2024 aluminium alloy," *Mater. Sci. Eng. A*, vol. 552, pp. 48–60, 2012.

[13] A. S. M. Handbook, *Volume 4*. 1991.

[14] M. Hajian and A. Assempour, "Experimental and numerical determination of

[Downloaded from i4c2023.iust.ac.ir on 2026-11-21]

[DOI: 10.22068/ase.2022.554]

forming limit diagram for 1010 steel sheet: a crystal plasticity approach," *Int. J. Adv. Manuf. Technol.*, vol. 76, no. 9–12, pp. 1757–1767, 2014.

[15] H. Rahimi, M. Sedighi, and R. Hashemi, "Forming limit diagrams of fine-grained Al 5083 produced by equal channel angular rolling process," *Proc. Inst. Mech. Eng. Part L J. Mater. Des. Appl.*, 2016: 1464420716655560.

[16] A. K. Ghosh, "The Influence of Strain Hardening and Strain-Rate Sensitivity on Sheet Metal Forming," *J. Eng. Mater. Technol.*, vol. 99, no. 1, p. 264, 1977.

[17] K. W. Neale and E. Chater, "Limit strain predictions for strain-rate sensitive anisotropic sheets," *Int. J. Mech. Sci.*, vol. 22, no. 9, pp. 563–574, 1980.

[18] S.M. Mirfalah-Nasiri, A. Basti, R. Hashemi, "Forming limit curves analysis of aluminum alloy considering the through-thickness normal stress, anisotropic yield functions and strain rate," *Int. J. Mech. Sci.*, vol. 117, pp. 93-101, 2016.

[19] M. Habibi, R. Hashemi, E. Sadeghi, A. Fazaeli, A. Ghazanfari, and H. Lashini, "Enhancing the Mechanical Properties and Formability of Low Carbon Steel with Dual-Phase Microstructures," *J. Mater. Eng. Perform.*, vol. 25, no. 2, pp. 382–389, 2016.

[20] F. Ozturk, E. Esener, S. Toros, and C. R. Picu, "Effects of aging parameters on formability of 6061-O alloy," *Mater. Des.*, vol. 31, no. 10, pp. 4847–4852, 2010.

[21] M. K. Sharma, J. Mukhopadyay, "Evaluation of Forming limit Diagram of Aluminium Alloy 6061-T6 at Ambient Temperature," Light Metals 2015, pp309-314, Springer.

[22] F. Djavanroodi, A. Derogar, "Experimental and numerical investigation of forming limit diagrams for Ti6Al4V titanium and Al6061-T6 aluminium alloys sheets," *Mater. Des.*, vol. 31, no. 10, pp. 4866-4875, 2010.

[23] D. Raja Satish, F. Feyissa, D. Ravi Kumar, "Cryorolling and warm forming of AA6061 aluminium alloy sheets," Mater. Manuf. Process., pp1-8, 2017.

[24] V.K. Barnwal, A. Tewari, K. Narasimban, "Effect of plastic anisotropy on forming behaviour of AA-6061 aluminium alloy sheet," J. Strain Anal. Eng., vol. 51, no. 7, pp. 507-517, 2016.

[25] J. Liu, M.J. Tan, A.E.W. Jarfors, Y. Aue-u-lan, S. Castagne, "Formability in AA5083 and AA6061 sheet alloy for light weight applications," Mater. Des., vol. 31, 566-570, 2010.

[26] M. Fallah Tafti, M. Sedighi, R. Hashemi, "Effects of Natural Aging Treatment on Mechanical, Microstructural and Forming Properties of Al 2024 Aluminum Alloy Sheets," Iranian Journal of Materials Science and Engineering, vol. 15 (4), 1-10, 2018.

Appendix

The FLDs were drawn for five considered temperatures.

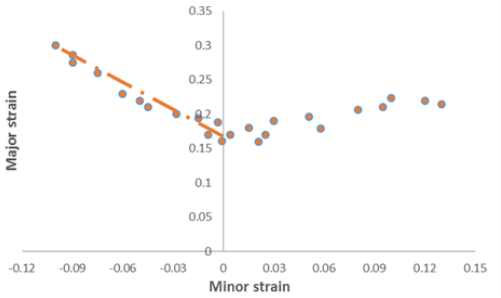


Fig. 1. Forming limit diagram just a little after solution treatment

[Downloaded from i4c2023.iust.ac.ir on 2026-11-21]

[DOI: 10.22068/ase.2022.554]

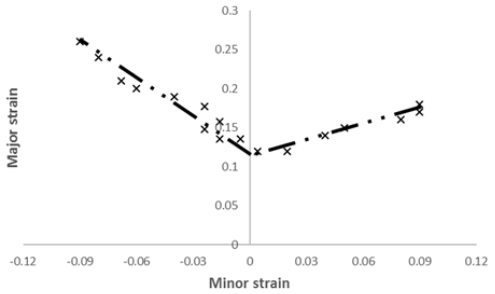


Fig. 2. Forming limit diagram in temperature 140 ºC

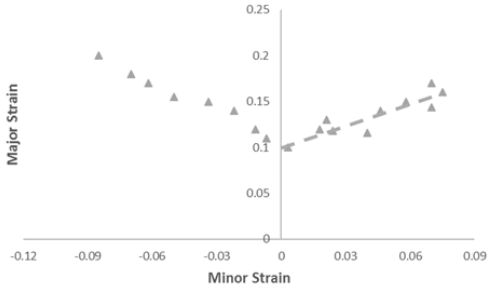


Fig. 3. Forming limit diagram in temperature 160 ºC

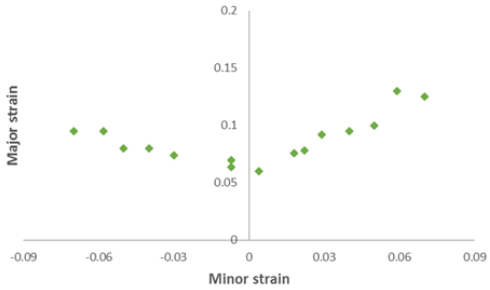


Fig. 4. Forming limit diagram in temperature 180 ºC (peak-aging)

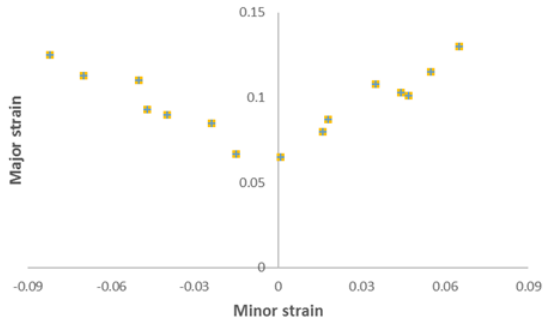


Fig. 5. Forming limit diagram in temperature 200 ºC (over-aging)

[Downloaded from i4c2023.iust.ac.ir on 2026-11-21]

[DOI: 10.22068/ase.2022.554]